c-Raf-1 RBD Associates with a Subset of Active v-H-Ras†

Masha Fridman, Francesca Walker, Bruno Catimel, Teresa Domagala, Edouard Nice, and Antony Burgess*

Ludwig Institute for Cancer Research, P.O. Box 2008, Royal Melbourne Hospital, Victoria 3050, Australia

Received May 30, 2000; Revised Manuscript Received September 11, 2000

ABSTRACT: Mutational analysis of the cRaf-1 *R*as *b*inding *d*omain (RBD) identified several point mutants with elevated Ras binding. Detailed examination of the binding kinetics of one mutant (A85K) suggests that it associates with a greater range of isomeric conformers of v-H-Ras than wt-RBD. At limiting v-H-Ras concentrations, saturation binding to A85K-RBD is higher than to wt-RBD. Notably, in assay systems where the RBD concentration is limiting, no difference exists between wt-RBD and A85K-RBD saturation levels in the presence of a sufficiently large molar excess of Ras. The inability of wt-RBD to saturate all bindable Ras/GTP (defined by its binding to A85K-RBD) suggests that Ras/GTP exists as several isoforms and that only a minority of these isoforms are capable of associating with wt-RBD. These findings provide the first experimental evidence in support of functionally distinct Ras/GTP isoforms. We also describe a novel analysis of such isoforms.

Ras proteins function as molecular "switches" in cell signaling, alternating between the active guanosine triphosphate (GTP)[1]-bound state and the inactive GDP-bound state (*1*). In its active, GTP-bound state, Ras transmits signals from stimulated cell surface receptors through several diverging pathways that regulate cellular processes. cRaf-1 is one of several cellular effectors of Ras that associate with active Ras/GTP but not with Ras/GDP (*1*, *2*). The minimal *R*as *b*inding *d*omain (RBD) of Raf has been narrowed down to an 80-residue sequence (*3*). The ability of RBD to distinguish between the active and the inactive forms of Ras led to its use as an activation-specific probe for Ras/GTP in cells (*4*).

Despite the high affinity of binding between Ras and wild-type RBD (*5*−*12*), their stoichiometric level of binding is surprisingly low. Recently Trier et al. (*13*) reported "sub-optimal" binding between the *g*reen *f*luorescent *p*rotein (GFP)-RBD fusion protein and activated cellular Ras. In a previous report, we identified RBD point mutants with elevated binding to v-H-Ras/GTP (*44*). The increased binding was unexpected because the concentration of RBD in the assay (1 μM) was well above the concentration expected to saturate Ras binding (*5*−*12*). Complex formation between Ras and Raf is reportedly very rapid, reaching equilibrium within 2 min (*14*), which is considerably less than the 15−30-min incubation times used in our previous binding assay (*44*). Under equilibrium binding conditions, v-H-Ras should be saturated by 1 μM wt-RBD or any other putative high-affinity mutant.

Several factors could be responsible for the observed difference in Ras saturation levels between wt-RBD and its mutants: different rates of dissociation for the Ras/RBD complex, different proportions of active protein in the RBD preparations, or binding of wt and mutant RBD constructs to distinct conformational subsets of Ras. Two recent NMR studies have shown that the RBD binding domains of Ras are dynamic and undergo slow interconversion between two or more conformers (*15*, *16*). It has been proposed that this conformational polymorphism may mediate the selection of Ras effectors such as Raf and GAP (*15*, *16*). Similarly, the set of Ras conformers binding wt-RBD may be distinct from the set of conformers that associate with the RBD mutants. A discrepancy in maximal binding levels could then arise if the mutants were capable of binding a greater proportion of total Ras than wt-RBD. We have investigated these alternative hypotheses, and our results support the notion that wt-RBD recognizes only a subset of Ras/GTP conformations.

EXPERIMENTAL PROCEDURES

Construction of RBD (*Residues 51*−*131*) *Mutants*. The mutants were constructed by PCR site-directed mutagenesis, using cRaf-1 cDNA (*17*) as a template. Oligonucleotides were synthesized incorporating the desired mutations as well as *Eco*RI restriction sites at the 5′ end to facilitate subcloning into the pGEX-2TH vector (kindly provided by Dr. H. Maruta) linearized with *Eco*RI. Mutations were verified by nucleotide sequencing

GST-RBD Expression and Purification. The procedure used for the expression and affinity purification of the glutathione S-transferase (GST)-RBD fusion proteins, using glutathione-coated Sepharose beads (Centre for Protein and Enzyme Technology, LaTrobe University), was performed essentially as described by Frangioni and Neel (*18*). Sepharose-linked GST-RBD fusion proteins were suspended in storage buffer (*18*) as a 1:1 suspension and then stored in 1-mL aliquots at −20 °C.

v-H-Ras Expression and Purification. v-H-Ras was expressed in NM522 cells (*17*) using the pUC8 expression

† Part of this work was carried out during the tenure of a grant from the Anti-Cancer Council of Victoria.

* Corresponding author telephone: 61-3-9341 3155; fax: 61-3-9341 3104; e-mail: tony.burgess@ludwig.edu.au.

[1] Abbreviations: RBD, Ras binding domain; wt, wild type; GST, glutathione *S*-transferase; GDP, guanosine diphosphate; GTP, guanosine triphosphate; GppNHp, guanylylimidodiphosphate; GTPγS, guanosine 5′-O-(thiotriphosphate); RU, refractive units.

10.1021/bi001224x CCC: $19.00
Published on Web 11/17/2000

vector(*19*), as previously described (*20*). v-H-Ras was released from bacterial cells into buffer A (64 mM Tris, 0.5 mM DTT, 10 mM $MgCl_2$, 0.01% *N*-octyl glucoside, 100 U/mL Trasylol, 1 mM PMSF, and 1 μM pepstatin, pH 8.0) using the procedure of Johnson and Hecht (*21*). The proteins released from cells were resolved on a 15 × 3 cm DEAE-Sepharose (Pharmacia) column with a 120-mL linear gradient of 0−0.4 M NaCl in buffer A (*22*). DEAE fractions containing v-H-Ras were subjected to 60% ammonium sulfate precipitation, size exclusion chromatography through a 2.6 cm × 100 cm Sephadex-G-100 column in buffer A containing 0.1 M NaCl, dialysis in buffer B (20 mM Tris, 5 mM $MgCl_2$, and 0.5 mM DTT), and finally elution through a MonoQ column with a 0−0.5 M NaCl gradient in buffer B. The progress of v-H-Ras purification was monitored by SDS−PAGE and GTPγS^{35} exchange.

Measurement of Protein Concentrations. The concentrations of proteins linked to Sepharose beads (GST-RBD as well as RBD-bound Ras) were determined by densitometry (Molecular Dynamics 300 series computing densitometer) of Coomassie-stained SDS−PAGE, using ImageQuant 3.3 (Molecular Dynamics) analysis. The concentration of purified Ras was determined using the Bio-Rad protein assay dye reagent (Bio-Rad).

v-H-Ras Storage, Preparation, and Labeling. The purified Ras was stored in exchange buffer (50 mM Tris-HCl, pH 7.5, 1 mM EDTA, 0.5 mg mL^{-1} BSA, 0.5 mM DTT, and 0.1 M NaCl) at −20 °C with a 12-fold molar excess of GTPγS. Prior to v-H-Ras labeling or nucleotide exchange, the concentration of excess cold GTPγS was reduced 20−40-fold using Centricon-10 filters (Amicon). v-H-Ras was labeled with GTPγS^{35} in exchange buffer for 15 min. The labeling reaction was terminated with 15 mM $MgCl_2$ (*20*, *23*−*25*), and unbound GTPγS^{35} was removed by elution through a PD-10 column (Pharmacia) in binding buffer (50 mM Tris-HCl, pH 7.5, 10 mM $MgCl_2$, 0.5 mg mL^{-1} BSA, 0.5 mM DTT, and 0.1 M NaCl).

Ras Bindability Assays. The measure of Ras bindability was given by its retention on sequential affinity columns, containing 1 mg of 0.7 mL^{-1} (40.7 μM) GST-RBD-coated Sepharose beads (Figure 2). A v-H-Ras/GTPγS (300 pg, 0.5 mL) labeled with GTPγS^{35} was loaded onto the first affinity column. Unbound protein was recovered by washing the column with 7.5 mL of binding buffer. The wash-through was collected and reloaded onto an identical second affinity column for another round of binding to RBD. The second column was washed with 5 mL of binding buffer to remove unbound Ras. To determine the amount of Ras bound to the beads, the contents of each column were suspended in up to 5.5 mL of binding buffer, and the radioactivity from 100-μL aliquots of the column suspensions was measured. This procedure was done in parallel for columns filled with GST-wt-RBD or GST-A85K-RBD.

Dissociation Assays. GTPγS^{35}-labeled v-H-Ras (2.3 μM) was incubated with 1.1 μM wt-RBD-GST or A85K-RBD-GST linked to glutathione-coated Sepharose beads. After a 75-min incubation period, the Sepharose beads were washed 3 times by centrifugation. Dissociation of the Ras/RBD complexes was commenced by adding 26 μM cold v-H-Ras/GTPγS and/or 287 μM GTPγS. At given intervals, aliquots (60 μL) were taken from the dissociation mix (500 μL starting volume) and washed 4 times by centrifugation. The radioactivity associated with the beads was determined using a Tri-CarbR liquid scintillation analyzer (Packard United Technologies).

v-H-Ras Saturation Radioassays. GTPγS^{35} labeled v-H-Ras (5 nM) was added to duplicate samples together with varying concentrations of RBD. After a 90-min incubation, the beads were washed by centrifugation in binding buffer, and the radioactivity associated with the beads was measured.

SDS−PAGE Saturation Assays. Complexes of v-H-Ras and GTPγS, GTP, or GppNHp were obtained by incubating 0.67 mM nucleotide and the required amount of Ras in exchange buffer. Nucleotide exchange was terminated by the addition of 15 mM $MgCl_2$. Aliquots of the exchange mix were added to samples containing R89L-GST, A85K-GST, or wt-RBD-GST linked to Sepharose beads. Nucleotide concentrations were adjusted to 152 μM in the binding reactions. The reactions were incubated for 15 min at room temperature. The beads were washed 3 times in binding buffer by centrifugation, and bound v-H-Ras was visualized on Coomassie-stained SDS−PAGE and quantified by densitometry.

GST-RBD Preparation for Biosensor Analysis. GST-RBD fusion proteins were released from agarose beads in 10 mM glutathione and 50 mM Tris, pH 8.0. Immediately prior to loading on the BIAcore surface, GST-RBD was purified on a Superose 12 HR 3.2/30 column (Pharmacia) in BIAcore buffer (10 mM HEPES, pH 7.4, 2 mM $MgCl_2$, 100 mM NaCl, and 0.005% (v/v) Tween 20).

BIACORE Assay Conditions. Biosensor analyses were performed using a BIAcore 2000 (Pharmacia Biosensor, Uppsala, Sweden). Sensor chip CM5, surfactant P20 (a 10% (v/v) solution of the nonionic detergent Tween 20), the amine coupling reagents (NHS, EDC, and ethanolamine), and the anti-GST monoclonal antibody were also obtained from Pharmacia Biosensor. The anti-GST mAb was immobilized onto the four channels of sensor surface using NHS/EDC coupling. GST-Raf mutants were captured onto immobilized anti-GST mAb. Ras and GST-RBD proteins were diluted in BIAcore buffer prior to analysis.

Immobilization of GST-RBD. The carboxymethyldextran-modified gold sensor surface was activated using a 35-μL mixture of *N*-ethyl-*N*′-dimethylaminopropylcarbodiimide (EDC, 200 mM) and *N*-hydroxysuccinimide (NHS, 50 mM) (*26*). The anti-GST mAb (50 μL at 40 μg/mL) was passed over the biosensor surface at 2 μL/min. The surface was blocked by injection of 50 μL of 1 M ethanolamine at pH 8.0 and washed using 50 μL of 10 mM NaOH at 5 μL/min. Solutions of the GST-RBD mutants in the BIAcore buffer were pumped over the immobilized anti-GST IgG at 4 μL/min.

Ras Binding onto Immobilized Raf Mutants. Excess nucleotide was removed from the v-H-Ras preparation by elution through a MonoQ column. v-H-Ras in BIAcore buffer (2.5−9 μM) was passed over RBD consructs on the BIAcore surfaces at 5 μL/min. Dissociation was monitored in BIAcore buffer for 360 s at the same flow rate. The surface was regenerated between injections using 40 μL of 10 mM NaOH. After desorption, fresh batches of GST-RBD mutants were recaptured onto immobilized anti-GST mAb.

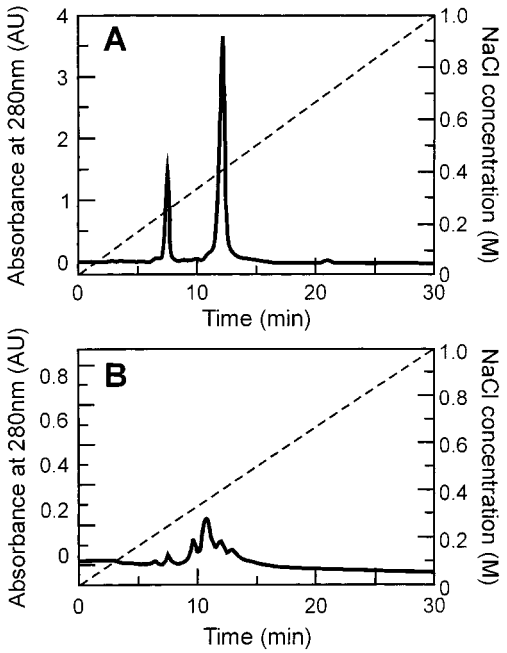

FIGURE 1: Purity and stability of Ras preparations. MonoQ elutions were carried out in a 30-min 0−1.0 M NaCl gradient in 20 mM Tris and 5 mM $MgCl_2$. (A) MonoQ profile of the Ras/GTPγS preparation, which had been stored with a 12-fold molar excess of GTPγS in exchange buffer at −20 °C for approximately 1 yr. The first peak in the profile corresponds to the elution of GTPγS. The purified v-H-Ras was stored at −20 °C in a 12-fold molar excess of GTPγS. In all experiments described here, the same preparation of v-H-Ras was used. (B) MonoQ profile of the Ras/GTPγS preparation, which had been depleted of excess GTPγS by buffer exchange on a Centricon-10 concentrator (Amicon) and stored in exchange buffer at −20 °C for approximately 1 yr.

Determination of Affinity Constants. The association and dissociation rate constants were calculated using NLLS analysis (*27*). The goodness of fit between experimental data and fitted curves was obtained for nonlinear least-squares fitting by χ^2 analysis using

$$\chi^2 = \frac{1\Sigma^n(r_f - r_x)^2}{n - p}$$

where r_f is the fitted value at a given point, r_x is the experimental value at the same point, n is the number of data points, and p is the number of degrees of freedom.

RESULTS

Purity of v-H-Ras. The v-H-Ras/GTPγS complex was purified to homogeneity using anion-exchange HPLC (Figure 1A). The presence of excess nuleotide appeared to stabilizes v-H-Ras during freezing/thawing. v-H-Ras, which had been stored frozen without excess nucleotide, has a heterogeneous MonoQ elution profile (Figure 1B).

Ras Bindability. The bindability of v-H-Ras in our preparation was determined by measuring the retention of labeled Ras on a series of affinity columns filled with either wt-RBD- or A85K-RBD-coated Sepharose beads. Table 1 shows the proportions of v-H-Ras/GTPγS^{35} retained on the columns. A total of 75% of the starting material was retained on A85K-RBD column 1; 25% of the total radioactivity in the wash-through from A85K-RBD column 1 bound to a second A85K-RBD column. On the basis of its retention on the tandem A85K-RBD affinity columns, the bindable portion of the v-H-Ras preparation was determined to be at least 82%. In contrast, only 3×10^6 cpm or 10.7% of the v-H-Ras/GTPγS^{35} was bound to the wt-RBD column 1. The unbound protein was loaded onto wt-RBD column 2, where less than 5% of the radioactivity was retained. Thus, less than 15% of the total Ras bound the wt-RBD, 6-fold less than the amount of v-H-Ras bound to the A85K-RBD columns. The marked reduction in Ras binding to the second column, relative to the first, is likely to be due to the depletion of bindable v-H-Ras rather than the dilution factor since the concentration of RBD in the columns was approximately 40 μM, well in excess of the published K_d (15−160 nM; *5*−*12*).

Table 1: Proportion of v-H-Ras/GTPγS^{35} Bound to wt-RBD or A85K-RBD Affinity Columns

	proportion of bound v-H-Ras[a] (%)	
	wt-RBD	A85K-RBD
v-H-Ras bound to column 1	10.5	75
v-H-Ras bound to column 2	4.8	25
total bound v-H-Ras	15.0	82

[a] The radioactivity of the starting material corresponded to 28.5×10^6 cpm 300 μg^{-1} of Ras/GTPγS.

The binding of Ras to the A85K-RBD columns provided an upper limit of bindability, defining the "active" fraction of Ras in this preparation as at least 82%. The dramatically lower level of bindability to wt-RBD columns confirmed our previous data,[2] showing a difference in the levels of Ras binding to wt-RBD and A85K-RBD.

Dissociation of Ras from wt-RBD and A85K-RBD. v-H-Ras/GTPγS^{35} dissociation from wt-RBD or A85K-RBD in the presence of excess unlabeled v-H-Ras/GTPγS is shown in Figure 2. The results of three separate experiments are superimposed in each graph. Despite the increased overall binding of Ras to A85K-RBD (Table 1), Ras dissociates faster from A85K-RBD than from wt-RBD (Figure 2A). After 10 min, 65% of Ras dissociated from wt-RBD, compared with 80% for A85K-RBD. Both dissociation profiles consist of two phases: a very rapid dissociation in the first 3 min, followed by a slower release. The second, slow phase is probably due to the release of labeled GTPγS^{35} rather than Ras dissociation from RBD: the slopes for the second phase correlate with GTPγS^{35} exchange (Figure 2B). There is no difference in GTP exchange between the samples containing A85K-RBD or wt-RBD (Figure 2B). Previous studies also reported a rapid dissociation rate for the Ras/wt-RBD complex (*6*, *12*): the majority of wt-RBD-bound Ras was displaced in 3 min (*6*), and the lifetime of the RBD/Ras complex in vitro was estimated to be 50−100 ms (*12*). The results in Figure 2 show that the elevated binding of A85K-RBD to Ras is not the result of stronger interactions of Ras with A85K-RBD.

Saturation Binding of v-H-RAS to wt-RBD and A85K-RBD. v-H-Ras saturation profiles for wt-RBD and A85K-RBD are illustrated in Figure 3. The binding of v-H-Ras/GTPγS^{35} to increasing concentrations of GST-wt-RBD and GST-A85K-RBD fusion proteins saturates at two different levels (Figure 3). The concentrations of wt-RBD and A85K-RBD required for half maximal binding are 130 and 140 nM, respectively. Therefore, under the conditions of the assay

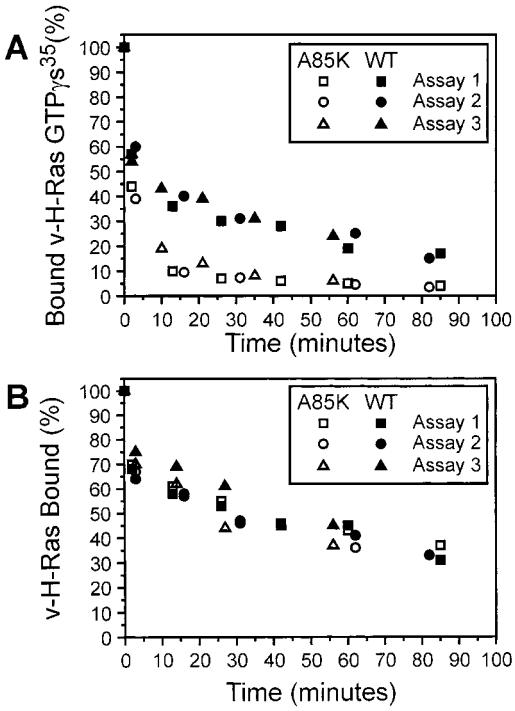

FIGURE 2: Dissociation of Ras from wtRBD and A85K-RBD. The dissociation of labeled v-H-Ras/GTPγS^{35} from wtRBD or A85K-RBD in the presence of excess unlabeled (A) 26 μM v-H-Ras/GTPγS and 287 μM GTPγS or (B) 287 μM GTPγS alone was carried out. The results from three separate experiments are superimposed.

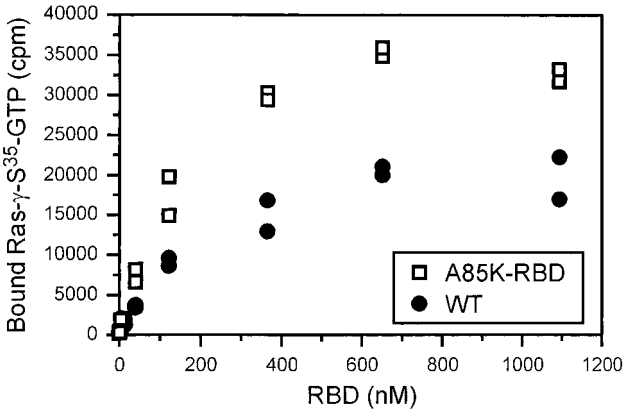

FIGURE 3: v-H-Ras saturation binding curves. Increasing concentrations of wtRBD or A85K-RBD were used to bind GTPγS^{35}-labeled v-H-Ras. The null R89K−RBD mutant (*33*) was used to measure nonspecific binding, which accounted for 0.05% of total counts.

wt-RBD and A85K-RBD have very similar apparent binding affinities for v-H-Ras.

Although the increased binding of v-H-Ras/GTPγS^{35} to wt-RBD and A85K-RBD was consistently observed, the magnitude of the increase varied between 2- and 5-fold, as if the proportion of total Ras capable of binding wt-RBD varied. The difference in wt-RBD and A85K-RBD binding was even more pronounced with v-H-Ras/GTPγS preparations stored at −20 °C in the absence of excess nucleotide: under these conditions 20−40-fold more v-H-Ras/GTPγS bound to A85K-RBD than to wt-RBD (data not shown). The mechanism through which excess nucleotide can affect Ras binding to wt-RBD has not been elucidated.

Affinity Determination by Biosensor Analysis. The BIAcore biosensor technology (*28*) measures small changes in refractive index at, or near to, the gold sensor surface (*29*). The change in mass as a ligand binds to or dissociates from its binding partner is monitored readily. The BIAcore 2000 biosensor used in these experiments permits parallel analysis of test samples on four different sensor channels. This allowed direct comparison of the binding characteristics of purified v-H-Ras with four GST-RBD mutants. GST-RBD constructs were captured by anti-GST monoclonal antibodies (BIAcore, Pharmacia) immobilized (*30*) onto the sensor surface (see Figure 4A), thus immobilizing RBD proteins in a defined orientation.

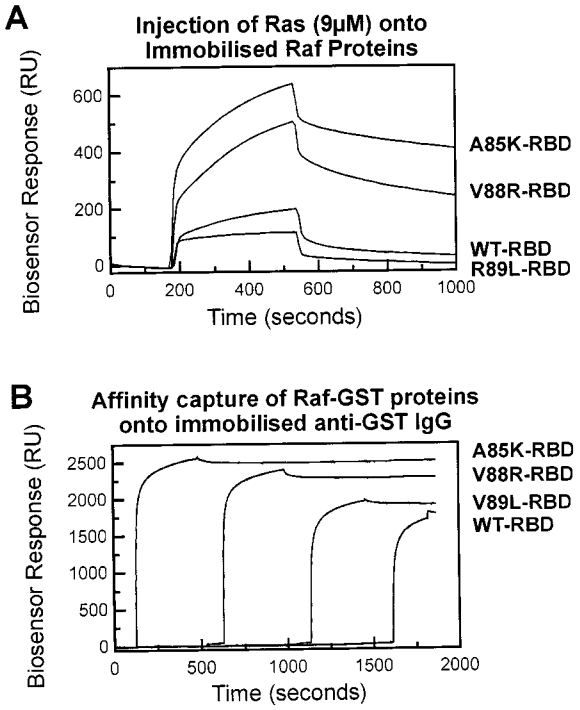

FIGURE 4: Biosensor analysis of Ras/RBD binding. (A) Monomeric RBD-GST (eluting after 17 min) was isolated by SEC immediately prior to immobilization on the biosensor surface. (B) Capture of GST-RBD mutants onto immobilized anti-GST IgG. WtRBD-GST, A85K-RBD-GST, V88R-RBD-GST, and R89L-RBD-GST were injected over the anti-GST IgG immobilized onto the four channels of the sensor chip. The levels of immobilization obtained were as follows: channel 1, 2493 RU of A85K-RBD-GST (approximately 2.5 ng/mm^2); channel 2, 2290 RU of V88R-RBD-GST (approximately 2.3 ng/mm^2); channel 3, 1819 RU of R85L-RBD-GST (approximately 1.8 ng/mm^2); channel 4, 1722 RU of wt-RBD-GST (approximately 1.7 ng/mm^2). (C) Biosensor analysis of the interaction between Ras and immobilized RBD-GST fusion proteins.

The amount of v-H-Ras bound to wt-RBD, V88R-RBD, and A85K-RBD increased in that order (Figure 4A). However, the amount of RBD protein captured onto immobilized anti-GST IgG was not uniform in all channels (Figure 4B). The binding of v-H-Ras/GTPγS was therefore expressed in terms of the molar binding activity (MBA) (*31*, *32*) rather than in absolute terms. R89L-RBD was used as a negative control (*33*).

Table 2 shows the changes in MBAs for wt-, A85K-, and V88R-RBDs with increasing concentrations of Ras. The difference in binding levels was still apparent: a smaller proportion of wt-RBD than A85K-RBD or V88R-RBD was associated with Ras. Since GST-RBD proteins have the same orientation, the observed differences in the binding of Ras to different RBD constructs reflected the impact of point mutations on binding and not immobilization problems. Nor

Table 2: Molar Binding Activities (MBA)[a] of wt and Mutant RBDs Immobilized on the Sensor

	L89R			wt			V88R			A85K		
[Ras] (μM)	RBD (RU)	Ras (RU)	MBA	RBD (RU)	Ras (RU)	MBA	RBD (RU)	Ras (RU)	MBA	RBD (RU)	Ras (RU)	MBA
2.5	1653	73		1454	84	0.011	2033	232	0.12	2191	249	0.12
4.5	1619	157		1598	185	0.027	2166	428	0.19	2175	443	0.20
7.0	1626	133		1476	168	0.036	2267	413	0.19	2098	436	0.22
9.0	1819	116		1722	198	0.070	2290	507	0.26	2493	641	0.32
13.5	1859	177		1722	366	0.17	2290	665	0.32	2297	645	0.31
22.5	1820	386		1618	548	0.15	2060	814	0.32	2149	810	0.31

[a] MBA = (amount of Ras bound [RU]) × (GST-RBD molecular mass)/(amount of immobilized GST-RBD [RU]) × (Ras molecular mass).

Table 3: Summary of Kinetic Analysis of Biosensor Binding Data for Interactions between v-H-Ras/GTPγS and RBD Constructs

Ras (μM)	RBD	$k_{a1} \times 10^{-3}$ ($M^{-1}s^{-1}$)	$k_{d1} \times 10^{3}$ (s^{-1})	$K_{d1} \times 10^{-6}$ (M)	$k_{a2} \times 10^{-3}$ ($M^{-1}s^{-1}$)	$k_{d2} \times 10^{4}$ (s^{-1})	$K_{d2} \times 10^{-6}$ (M)
22.5	K85	1.7	5.5	0.71	1.1	1.9	0.20
	R88	2.2	5.5	2.5	0.5	1.6	0.33
	wt	1.4	15	11	0.15	2.4	1.7
13.5	K85	4.4	5	1.1	0.6	2	0.33
	R88	2.5	9.1	3.3	0.6	2.8	0.59
	wt	4.2	14	3.3	0.14	2.1	1.7
9.0	K85	6	4.5	0.77	0.5	1.7	0.33
	R88	1.8	5.8	3.3	0.5	3.6	1
	wt	2.3	15.8	10	0.4	3.5	1
7.0[a]	K85	3.6	25	6.6	1	4	0.4
	R88	1	16	16.6	1.5	7	0.58
	wt						
4.5[a]	K85	6.7	5	0.77	1.1	1.9	0.17
	R88	4.1	7	4	0.9	3.9	0.43
	wt						

[a] Low signal intensity for wt-RBD at 4.5 and 7 mM Ras precluded kinetic analysis.

was there a difference in the proportion of correctly folded protein in the two key RBD preparations (wt and A85K-RBD) since under appropriate conditions both were able to bind equal amounts of Ras (Figure 6 and Table 4).

The apparent association rate (k_a), dissociation rate (k_d), and the resulting K_d were determined from the binding curves using nonlinear least-squares analysis (NLLS) (*27*) of the primary data as previously described (*34*−*36*). The apparent binding constants were derived using a double-exponential form of the rate equation applied to the total association or dissociation phase (Table 3). This type of analysis results in two values for the dissociation phase ($k_{d1}$and k_{d2}) and also for the association phase (k_{a1} and k_{a2}). However, the relative amplitudes obtained from this analysis suggested than one set of values, corresponding to k_{a2} and k_{d2}, predominated, i.e., more than 80% of the binding and dissociation signal was due to these processes.

The average affinities and their standard deviations for the v-H-Ras/RBD interactions, estimated from $k_{a2}$and k_{d2} (Table 3) were as follows: $K_{d2(A85K\text{-}RBD)} = 0.29 \pm 0.10$ μM; $K_{d2(V88R\text{-}RBD)} = 0.59 \pm 0.26$ μM; $K_{d2(wt\text{-}RBD)} = 1.5 \pm 0.40$ μM. Thus, the biosensor data suggests a 5-fold difference between wt-RBD and A85K-RBD in the affinity for Ras. This difference is not apparent from the saturation curve (Figure 4). The K_d estimate from the biosensor data for the wt-RBD/Ras interaction (1.5 ± 0.40 μM) is an order of magnitude higher than our estimate from the saturation curve in Figure 3 (140 nM). The K_d value for the A85K mutant ($K_{d2} = 0.29 \pm 0.1$ μM) was much closer to the estimate from the saturation curve in Figure 4 ($K_d = 0.13$ μM).

Models of Ras/RBD Binding. While the binding of v-H-Ras to wt-RBD is consistently lower than to A85K-RBD, the magnitude of this difference varied largely due to variability in Ras binding to wt-RBD. These results suggest that wtRBD could only bind an unstable minor subset of Ras, where as the A85K mutant was less selective. The notion that RBD mutants select different subsets of the Ras population for binding could be tested experimentally.

Two binding models have been tested. In the first model, the difference between wt- and A85K-RBD is assumed to be due solely to different affinities for a single species of Ras. If this were the case, any difference in binding levels would be maintained regardless of whether the concentration of Ras were limiting or, conversely, the concentration of RBD were limiting. The expected saturation profiles under this model are shown in Figure 5A: the higher binding affinity of the Ras/A85K-RBD complex would be reflected by the lower concentrations of A85K-RBD (Figure 5A-i) and Ras (Figure 5A-ii) required to achieve half-maximal binding.

In the model that assumes multiple conformers of Ras (the isomeric model), wt-RBD and A85K-RBD select different sets of Ras isoforms for binding. In this case, reversing RBD and Ras concentration levels would not produce the same saturation levels (Figure 5B). Where Ras/GTP is limiting and RBD in excess (Figure 5B-i), two different maximal Ras-binding levels would be evident in wt-RBD and A85K-RBD saturation curves. The reactions would effectively proceed as if there were a higher concentration of Ras in the A85K-RBD samples, because A85K-RBD is able to associate with a greater proportion of Ras molecules than wt-RBD. In this scheme, a larger proportion of total Ras is capable of binding A85K-RBD than wt-RBD, resulting in an apparently lower affinity constant for wt-RBD that for A85K-RBD. According

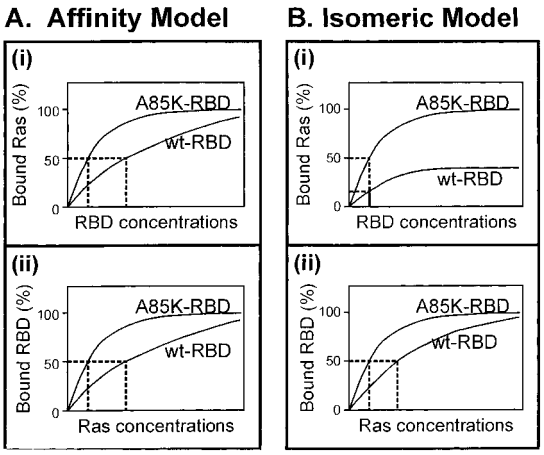

FIGURE 5: Expected saturation profiles for two binding models. (A) Affinity model of Ras/RBD binding based on a higher affinity of A85K-RBD for a single conformational form of Ras. (i) The expected saturation profiles for Ras with increasing concentrations of wtRBD and A85K-RBD. (ii) The expected saturation profiles for wtRBD and A85K-RBD with increasing concentrations of Ras. (B) Isomeric model of Ras/RBD binding based on preferential binding between wtRBD and a minor conformational subset of Ras. (i) The expected saturation profiles for Ras with increasing concentrations of wtRBD and A85K-RBD. (ii) The expected saturation profiles for wtRBD and A85K-RBD with increasing concentrations of Ras.

to the model of Ras isomers, it should be possible to saturate both wt and mutant RBD to the same level at a sufficiently high concentration of Ras and a limiting concentration of RBD (Figure 5B-ii).

Of the binding experiments so far described, the BIAcore assay was the only one where the concentration of Ras was in excess of RBD. In agreement with the isomeric model, the K_{d2} estimate for the wt-RBD/Ras interaction on the sensor surface (1.5 μM) was an order of magnitude higher than the estimate of 0.14 μM from the saturation curve in Figure 3, where wt-RBD was in excess of Ras. One aspect of the BIAcore data, however, seemed inconsistent with the model of multiple Ras conformers. Two different binding levels were still present with limiting RBD and excess Ras concentrations of up to 22.5 μM (Table 2). In the isomeric model, a high concentration of Ras is expected to saturate both wt-RBD and A85K-RBD to the same level (Figure 5B-ii). We considered the possibility that, even at a concentration as high as 22.5 μM, the putative minor bindable component of Ras was still insufficient to saturate wt-RBD. To validate this model, it was necessary to find ways of enriching this bindable component.

Effect of GTP Analogues on Ras Binding. One possible way to enrich the fraction of Ras that associates with wt-RBD was suggested by the results from two previous NMR studies (*15*, *16*). Different GTP analogues were reported to influence the equilibrium between interconvertible isomers of Ras and to alter the abundance of specific Ras isomers. We prepared Ras complexes with three different nucleotides (GTP, GTPγS, and GppNHp) in the attempt to enrich the putative portion of Ras that could bind wt-RBD. The results of biosensor experiments using these Ras preparations are summarized in Table 4. The most notable finding was that 25 μM Ras/GTP is able to bind wt-RBD and A85K-RBD at very similar levels ($MBA_{A85K\text{-}RBD}/MBA_{wt\text{-}RBD} = 1.1$). The discrepancy in binding levels between wt-RBD and V88R-RBD was still evident, although less pronounced with GTP-bound Ras ($MBA_{V88R\text{-}RBD}/MBA_{wt\text{-}RBD} = 1.4$) than for GTP$\gamma$S and GppNHp-bound Ras (with respective ratios of 1.7 and 1.8).

Table 4: Effect of Ras-Bound Nucleotide on RBD Binding[a]

	GTPγS		GTP		GppNHp	
	MBA[b]	MBA (mutant)[c] MBA (wt)	MBA	MBA (mutant) MBA (wt)	MBA	MBA (mutant) MBA (wt)
wt	0.24	1.0	0.36	1.0	0.31	1.0
A85K	0.36	1.5	0.41	1.1	0.45	1.5
V88R	0.40	1.7	0.50	1.4	0.56	1.8

[a] V-H-Ras bound to either GTPγS, GTP, or GppNHp was passed through four channels over biosensor surfaces. GST-RBD constructs were linked to the surfaces through an anti-GST mAb. The association of V-H-Ras with R89R-RBD-GST was used to define nonspecific bindng. [b] Molar binding activities determined from Biosensor profiles. [c] MBA ratios relative to the MBA of wt-RBD.

The results in Table 4 are consistent with the existence of bindable Ras conformers, which are affected by different nucleotides. However, the discrepancy in binding levels could also be interpreted as an artifact associated with nonphysiological GTP analogues. To demonstrate the heterogeneous nature of Ras, it was important to illustrate the disparity in binding levels for Ras/GTP in the presence of excess wt-RBD and A85K-RBD (see Figure 6), in the same experimental system. It is not possible to perform this experiment by immobilizing Ras on the sensor surface. The results would be difficult to interpret because the procedure itself could create an artificially heterogeneous population of Ras due to variability in the surface orientation of the immobilized molecules.

Effect of Ras:RBD Concentration Ratios on Binding. It is possible to reverse the Ras/RBD concentration ratios in a simple in vitro binding experiment. There is no need to label Ras because at saturation levels of binding, the protein concentrations can be sufficiently high to visualize their association by SDS−PAGE. Using this technique, we tested RBD/Ras binding at three different ratios. Both wt-RBD and A85K-RBD reach similar saturation levels with a large excess of Ras. In the presence of a 19-fold molar excess of Ras, wt-RBD and A85K-RBD precipitated equivalent amounts of v-H-Ras/GTP or v-H-Ras/GppNHp (Figure 6A). The binding of Ras/GTPγS was still lower for wt-RBD. It is important to note that the results in Figure 6A also illustrate that the wt-RBD and A85K-RBD preparations contain similar fractions of active protein, given that both were saturated at the same level with excess Ras/GTP. Therefore, we can rule out the possibility that differences in the quality of the RBD preparations account for the discrepancy in binding levels in the previous experiments.

At similar concentrations of Ras and RBD (8 and 5.6 μM, respectively) approximately 2-fold more Ras was bound to A85K-RBD than to wt-RBD (Figure 6B). In this instance, the nature of the GTP analogue in complex with v-H-Ras had little effect on the amount of RBD-bound Ras. Similarly, at a limiting concentration of Ras (Figure 6C), there is an obvious difference in the amount of Ras associated with wt-RBD and A85K-RBD, regardless of the specific nucleotide bound to Ras. It was difficult to quantify the intensities of the v-H-Ras bands in Figure 6C because of the high

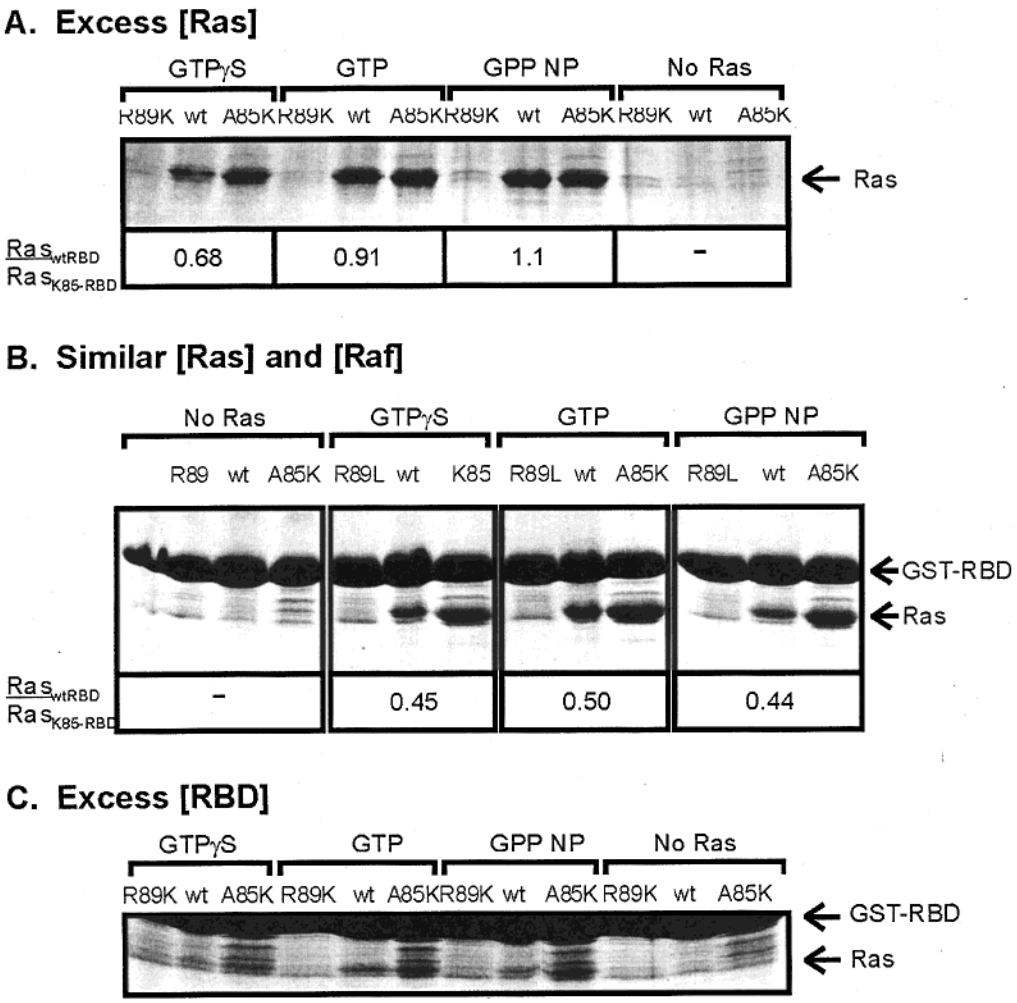

FIGURE 6: Effect of RBD and Ras concentration ratios on overall Ras/RBD binding. The reactions were carried out with v-H-Ras in complex with GTP, Ras/GTPγS, or Ras/GppNHp. The relative amount of Ras bound to each RBD construct was estimated by densitometry where possible. The ratios of wtRBD-bound Ras relative to A85K-RBD-bound Ras are shown. (A) Excess concentrations of RBD relative to Ras: [Ras] = 1.5 μM; [RBD] = 5.7 μM. (B) Similar concentrations of Ras and RBD: [Ras] = 8 μM; [RBD] = 5.6 μM. (C) Excess concentration Ras relative to RBD: [Ras] = 11.2 μM; [RBD] = 0.6 μM.

background from the overloaded RBD samples, which contained 50 μg of protein/RBD band.

The binding pattern for Ras/GTP and Ras/GppNHp corresponds to the multiple conformers model illustrated in Figure 6. Although Ras can saturate both wt-RBD and A85K-RBD at the same level of binding, the two RBD constructs saturate v-H-Ras at two separate levels. This finding suggests that Ras exists as a heterogeneous population of isomers and that a large proportion of active Ras is unavailable for binding wt-RBD. Importantly, the model applies to Ras in complex with GTP, which is the physiological nucleotide.

DISCUSSION

In the past, there have been few estimates of Ras bindability. Direct Ras-Raf binding assays estimated that 5−10% (*37*) and 40% (*8*) of Ras can be precipitated with a Raf-GST fusion protein. These rather low estimates of Ras bindability could be attributed to Ras dissociation during a series of washes required to separate bound from free Ras. Another study by Warne et al. reported 100% Ras bindability to the amino terminal region of cRaf-1 (*14*), which is difficult to reconcile with the hydrolysis that occurs during a 3-h binding reaction containing GTPαP^{32}-labeled wt-H-Ras.

The proportion of bindable Ras in our preparation was determined by passing labeled Ras through a series of RBD affinity columns: 82% of Ras binds the A85K-RBD columns, while only 15% of Ras binds the wt-RBD columns. Therefore, the A85K-RBD mutant defines the level of bindability for active Ras above the level of wt-RBD binding. There is no correlation between the increased binding of v-H-Ras to A85K-RBD and the dissociation rate, since the dissociation of v-H-Ras from A85K-RBD is faster than from wt-RBD. Nor could the difference in binding be attributed to different fractions of active protein in the RBD preparations, given that both wt-RBD and A85K-RBD are saturated at equivalent levels in the presence of a large excess of Ras. The observed binding pattern is consistent with the existence of conformational isomers in the purified v-H-Ras preparation, which are capable of binding A85K-RBD but not wt-RBD.

We tested the possibility that wt-RBD and A85K-RBD bind distinct subsets of the Ras population by changing the concentration ratios of v-H-Ras and RBD in a single assay system. When the concentration of RBD was in excess of v-H-Ras, A85K-RBD saturated v-H-Ras at a higher level than wt-RBD. However, when the concentration of Ras was

in excess of RBD, both wt-RBD and A85K-RBD precipitated equal amounts of v-H-Ras/GTP. These observations indicate that at a sufficiently high concentration of v-H-Ras, the amount of the minor isomeric subset of v-H-Ras that can associate with wt-RBD is adequate to saturate wt-RBD. At the same time, the inability of wt-RBD to saturate all bindable Ras (defined by its binding to A85K-RBD) indicates that Ras/GTP exists in several bindable isoforms and that only a minority of these isoforms is capable of associating with wtRBD.

It is possible that the presence of a positive charge in RBD position 85 facilitates the conversion of Ras to a bindable form. In the future, it may be possible to estimate the free energy barrier between the bindable and nonbindable forms of Ras from a time course of wt-RBD and A85K-RBD binding reactions.

Two previous NMR studies (*15*, *16*) described the conformational isomerism of Ras. Geyer et al. reported the existence of two conformational states with different binding characteristics for the β- and γ-phosphates of GppNHp (a GTP analogue) (*15*). In a Ras/GppNHp/RBD complex, only one conformational state (state 2) is evident. Another putative target of Ras, AF6, was also found to stabilize conformational state 2 upon binding, similarly to RBD (*38*). On the other hand, GAP appeared to interact with both conformational states of Ras, increasing the interconversion between them and favoring an increase in the population of state 1 (*15*). A different NMR analysis showed that the backbone amide resonances of amino acid residues in the *switch I* and *switch II* regions of Ras displayed extreme band broadening in the active Ras/GTP complex but not in the inactive Ras/GDP complex (*16*). This broadening suggested that the switch regions in the active complex undergo slow interconversion between two or more stable conformers (*16*).

Several studies have examined the kinetics of binding between Ras and GTP analogues (*8*, *39*−*43*). Geyer et al. detected conformational differences between GTP-, GTPγS-, and GppNHp-bound Ras by NMR (*15*): the conformation stabilized in the Ras/RafRBD complex (state 2) was equivalent to a prominent conformation of GppNHp/Ras in solution. State 2 is barely detectable in solutions of GTPγS/Ras (*15*). However, there have been no studies assessing the possible effects of the analogues on the interactions between Ras and Raf. Our results show that the nature of the nucleotide associated with Ras influences the abundance of wt-RBD-bindable Ras. The highest Ras/wt-RBD binding was observed with the physiological nucleotide (GTP), and the lowest was observed with GTPγS (Table 4 and Figure 6A). Perhaps specific GTP analogues affect the equilibrium between the interconvertible isomers of Ras and, hence, change the proportion of specific isoforms in the total Ras population.

Geyer et al. (*15*) and Ito et al.(*16*) proposed that Ras isoforms may serve to discriminate among multiple Ras effectors (*1*, *2*) for binding. The distinction between the wt-RBD and A85K-RBD probes could be exploited in examining the importance of Ras/GTP conformers to the interaction of Ras with its effectors. It is interesting to consider the possible roles for other Ras binding proteins (GAP, PI3K, NF-1, etc. (*1*, *2*)). Perhaps they are capable of modifying the conformational equilibrium for Ras and, consequently, the amplitude of particular cell surface signals.

De Rooij and Bos (*4*) reported the use of wt-RBD as a probe for activated Ras in cells (*4*). In prelimenary experiments (*44*), we demonstrated that A85K-RBD is 5-fold more effective as a probe for total activated Ras. The findings outlined in this report explain the reasons for the efficiency of A85K-RBD binding. Since wt-RBD associates with only a minor conformational subset of Ras/GTP, whereas A85K-RBD is capable of detecting the majority of active Ras, A85K-RBD may give a better indication of total cellular Ras/GTP than wt-RBD.

The analytical method used to identify distinct functional subsets of v-H-Ras in this report could be applied to other proteins with multiple binding partners. It would be interesting to examine to what extent conformational isomerism, rather than competitive binding, accounts for the choice of specific effectors in protein binding reactions.

REFERENCES

1. Campbell, S. L., Khosravi-Far, R., Rossman, K. L., Clark, G. J., and Der, C. J. (1998) *Oncogene 17*, 1395−413.
2. Joneson, T., and Bar-Sagi, D. (1997) *J. Mol. Med. 75*, 587−93.
3. Vojtek, A. B., Hollenberg, S. M., and Cooper, J. A. (1993) *Cell 74*, 205−14.
4. de Rooij, J., and Bos, J. L. (1997) *Oncogene 14*, 623−5.
5. Herrmann, C., Martin, G. A., and Wittinghofer, A. (1995) *J. Biol. Chem. 270*, 2901−5.
6. Gorman, C., Skinner, R. H., Skelly, J. V., Neidle, S., and Lowe, P. N. (1996) *J. Biol. Chem. 271*, 6713−9.
7. Scheffler, J. E., Waugh, D. S., Bekesi, E., Kiefer, S. E., LoSardo, J. E., Neri, A., Prinzo, K. M., Tsao, K. L., Wegrzynski, B., Emerson, S. D., et al. (1994) *J. Biol. Chem. 269*, 22340−6.
8. Hwang, M. C., Sung, Y. J., and Hwang, Y. W. (1996) *J. Biol. Chem. 271*, 8196−202.
9. Block, C., Janknecht, R., Herrmann, C., Nassar, N., and Wittinghofer, A. (1996) *Nat. Struct. Biol. 3*, 244−51.
10. Herrmann, C., Ahmadian, M. R., Hofmann, F., and Just, I. (1998) *J. Biol. Chem. 273*, 16134−9.
11. Ohnishi, M., Yamawaki-Kataoka, Y., Kariya, K., Tamada, M., Hu, C. D., and Kataoka, T. (1998) *J. Biol. Chem. 273*, 10210−5.
12. Sydor, J. R., Engelhard, M., Wittinghofer, A., Goody, R. S., and Herrmann, C. (1998) *Biochemistry 37*, 14292−14299.
13. Trier, U., Olah, Z., Kleuser, B., and Schafer-Korting, M. (1999) *Pharmazie 54*, 263−8.
14. Warne, P. H., Viciana, P. R., and Downward, J. (1993) *Nature 364*, 352−5.
15. Geyer, M., Schweins, T., Herrmann, C., Prisner, T., Wittinghofer, A., and Kalbitzer, H. R. (1996) *Biochemistry 35*, 10308−20.
16. Ito, Y., Yamasaki, K., Iwahara, J., Terada, T., Kamiya, A., Shirouzu, M., Muto, Y., Kawai, G., Yokoyama, S., Laue, E. D., Walchli, M., Shibata, T., Nishimura, S., and Miyazawa, T. (1997) *Biochemistry 36*, 9109−19.
17. Fridman, M., Tikoo, A., Varga, M., Murphy, A., Nur, E. K. M. S., and Maruta, H. (1994) *J. Biol. Chem. 269*, 30105−8.
18. Frangioni, J. V., and Neel, B. G. (1993) *Anal. Biochem. 210*, 179−87.
19. Stein, R. B., Robinson, P. S., and Scolnick, E. M. (1984) *J. Virol. 50*, 343−51.
20. Tucker, J., Sczakiel, G., Feuerstein, J., John, J., Goody, R. S., and Wittinghofer, A. (1986) *EMBO J. 5*, 1351−8.
21. Johnson, B. H., and Hecht, M. H. (1994) *Biotechnology (N.Y.) 12*, 1357−60.
22. Gibbs, J. B., Sigal, I. S., Poe, M., and Scolnick, E. M. (1984) *Proc. Natl. Acad. Sci. U.S.A. 81*, 5704−8.
23. Hall, A., and Self, A. J. (1986) *J. Biol. Chem. 261*, 10963−5.

24. Hara, M., Tamaoki, T., and Nakano, H. (1988) *Oncogene Res. 2*, 325−33.
25. Mistou, M. Y., Cool, R. H., and Parmeggiani, A. (1992) *Eur. J. Biochem. 204*, 179−85.
26. Johnsson, B., Lofas, S., and Lindquist, G. (1991) *Anal. Biochem. 198*, 268−77.
27. O'Shannessy, D. J., Brigham-Burke, M., Soneson, K. K., Hensley, P., and Brooks, I. (1993) *Anal. Biochem. 212*, 457−68.
28. Liedberg, B., Lundstom, I., and Stenberg, E. (1993) *Sens. Actuators 11*, 63−72.
29. Lofas, S., and Johnsson, B. (1990) *J. Chem. Soc. Chem. Commun. 21*, 1526−8.
30. Nilsson, J., Larsson, M., Stahl, S., Nygren, P. A., and Uhlen, M. (1996) *J. Mol. Recognit. 9*, 585−94.
31. Johnsson, B., Lofas, S., Lindquist, G., Edstrom, A., Muller Hillgren, R. M., and Hansson, A. (1995) *J. Mol. Recognit. 8*, 125−31.
32. Catimel, B., Nerrie, M., Lee, F. T., Scott, A. M., Ritter, G., Welt, S., Old, L. J., Burgess, A. W., and Nice, E. C. (1997) *J. Chromatogr. A 776*, 15−30.
33. Fabian, J. R., Vojtek, A. B., Cooper, J. A., and Morrison, D. K. (1994) *Proc. Natl. Acad. Sci. U.S.A. 91*, 5982−6.
34. Nice, E. C., McInerney, T. L., and Jackson, D. C. (1996) *Mol. Immunol. 33*, 659−70.
35. Catimel, B., Nerrie, M., Lee, F. T., Scott, A. M., Ritter, G., Welt, S., Old, L. J., Burgess, A. W., and Nice, E. C. (1997) *J. Chromatogr. A 776*, 15−30.
36. Catimel, B., Scott, A. M., Lee, F. T., Hanai, N., Ritter, G., Welt, S., Old, L. J., Burgess, A. W., and Nice, E. C. (1998) *Glycobiology 8*, 927−38.
37. Chuang, E., Barnard, D., Hettich, L., Zhang, X. F., Avruch, J., and Marshall, M. S. (1994) *Mol. Cell Biol. 14*, 5318−25.
38. Linnemann, T., Geyer, M., Jaitner, B. K., Block, C., Kalbitzer, H. R., Wittinghofer, A., and Herrmann, C. (1999) *J. Biol. Chem. 274*, 13556−62.
39. Hattori, S., Ulsh, L. S., Halliday, K., and Shih, T. Y. (1985) *Mol. Cell Biol. 5*, 1449−55.
40. Finkel, T., Der, C. J., and Cooper, G. M. (1984) *Cell 37*, 151−8.
41. Manne, V., Yamazaki, S., and Kung, H. F. (1984) *Proc. Natl. Acad. Sci. U.S.A. 81*, 6953−7.
42. Feuerstein, J., Goody, R. S., and Wittinghofer, A. (1987) *J. Biol. Chem. 262*, 8455−8.
43. Rensland, H., John, J., Linke, R., Simon, I., Schlichting, I., Wittinghofer, A., and Goody, R. S. (1995) *Biochemistry 34*, 593−9.
44. Fridman, M., Maruta, H., Gonez, J., Walker, F., Treutlein, H., Zeng, J., Burgess, A. (2000) *J. Biol. Chem. 275*, 30363−71.

BI001224X